BBA - General Subjects 1861 (2017) 2304–2314

Contents lists available at ScienceDirect

BBA - General Subjects

journal homepage: www.elsevier.com/locate/bbagen

Conductive polymer-based bioelectrochemical assembly for *in vitro* cytotoxicity evaluation: Renoprotective assessment of *Salvia officinalis* against carbon tetrachloride induced nephrotoxicity

Evangelia Flampouri[a,*], Nefeli-Sofia D. Sotiropoulou[b], Sofia Mavrikou[a], Akrivi-Chara Mouzaki-Paxinou[c], Petros A. Tarantilis[b], Spyridon Kintzios[a]

[a] *Laboratory of Cell Technology, Department of Biotechnology, School of Food, Biotechnology and Development, Agricultural University of Athens, Iera Odos 75, 11855 Athens, Greece*

[b] *Laboratory of Chemistry, Department of Food Science and Human Nutrition, School of Food, Biotechnology and Development, Agricultural University of Athens, Iera Odos Street, 75, Athens 11855, Greece*

[c] *Laboratory of Ecology and Environmental Science, Department of Crop Science, School of Agriculture, Engineering and Environmental Science, Agricultural University of Athens, Iera Odos 75, Athens 11855, Greece*

ARTICLE INFO

Keywords:
Renal cells
Conducting polymer
Cell-based biosensor
Cytotoxicity
Carbon tetrachloride
Salvia officinalis

ABSTRACT

Background: The rise of organic electronics represents one of the most prominent technological developments of the last two decades, with its interface with biological systems highlighting new directions of research. The "soft" nature of conducting polymers renders them unique platforms for cell-based microdevices, allowing their implementation in drug discovery, pharmaceutical effect analysis, environmental pollutant testing *etc*.

Methods: Cellular adhesion, proliferation and viability experiments were carried out to verify the biocompatibility of a PEDOT conductive polymer surface. Cyclic voltammetry was employed for estimating the electrocatalytic activity of the renal cell/electrode interface. The nephrotoxicity agent CCl_4 and the medicinal plant *Salvia officinalis* were used on the proposed assembly. Renal cell viability was also assayed through the MTT assay.

Results: Renal cells were able to adhere and proliferate on the conducting polymer surface. Electrochemical responses of the polymer exhibited good correlation with cell number and CCl_4 concentration. Amelioration of the CCl_4-induced renotoxicity by co-incubation with *Salvia officinalis* extract was demonstrated by both the MTT assay and the electrode's capacitance.

Conclusions: A conducting polymer-based bioelectrochemical assembly was established for *in vitro* mammalian cytotoxicity/cytoprotection assessment, employing renal cell monolayers as the primary transducers for signal generation and biological sensing.

General significance: The knowledge on PEDOT mammalian cell biocompatibility and possible applications was expanded. The proposed interdisciplinary approach connects soft electronics with biology and could provide a useful tool for preliminary crude drug screening and bioactivity studies of natural products or plant extracts *in vitro*.

1. Introduction

The rise of organic electronics represents one of the most prominent technological developments of the last two decades, with its interface with biological systems being a dynamically emerging field that highlights new directions of research. Apart from their general advantages like low cost of materials, tunable electronic or optical properties, easy process ability, light weight, low environmental impact and potential for low cost [76,96], organic electronics are gaining momentum as remarkable transducers of biological events. The soft mechanical properties of many organics offer better compatibility with delicate biological tissues and cells than traditional electronic materials, while their ability to conduct ions in addition to electrons and holes opens up a new communication channel with biology [57,79].

Conducting polymers (CPs), typically employed in organic electronics, are polymeric materials, organic in nature that hold unique properties such as electrical conductivity, high electron affinity, low ionization potential and redox activity [9,94]. Additionally, their

* Corresponding author.
E-mail address: flampouri_kel@aua.gr (E. Flampouri).

http://dx.doi.org/10.1016/j.bbagen.2017.06.021
Received 21 February 2017; Received in revised form 23 June 2017; Accepted 26 June 2017
Available online 28 June 2017

plasticity, which allows them to act as excellent materials for immobilization of biomolecules, renders them unique biosensor platforms [8,38], while their ability to act as both sensing elements and transducers during biological recognition events, simplifies biosensor designs [2,9].

Among CPs, Poly (3,4ethylenedioxythiophene) (PEDOT) has become an established electronic material, holding the highest market share for conducting polymers in the capacitor market today [33]. PEDOT, which was found to be almost transparent in thin oxidized films, exhibits not only a high conductivity but also high stability in oxidized state and has been considered as perhaps the most stable conducting polymer currently available [26,42]. Due to its biocompatibility and similarity to biological compounds, PEDOT has been regularly used in bioengineering and biosensing applications [16,50,70,88]. PEDOT films have been widely demonstrated to support the adhesion and proliferation, among others, of fibroblasts [24], neural [41], neuroblastoma [6] and epithelial [14] cells.

Cell-based biosensors combine intact living cells with sensors or transducers for monitoring physiological changes in various cell types caused by internal or external stimuli [17,98]. Because of the complex nature of their biorecognition elements (whole living cells), they naturally encapsulate composite sensor arrays, providing a wide range of sensing capabilities and thus are expected to respond optimally to bioactive analytes [67]. Cell-based microdevices, including cell-based biosensors, are able to assess many cellular responses, such as adhesion, proliferation, integrity, migration, differentiation and signaling [25,36,43], in a manner that allows their implementation in drug discovery, pharmaceutical effect analysis, clinical practice, environmental pollutant testing, food safety *etc*. [11,30,54].

Plants have been used for their therapeutic properties for millennia [91], while natural products have long been served as critical stimuli for drug design [89]. Drug discovery from natural sources is an intrinsically complex process that necessitates highly integrated interdisciplinary research approaches [44]. Historically, drug screening relies principally on animal tests which are expensive, time consuming, low throughput and ethically provoking [5]. These limitations have stimulated continuous research on developing cell-based platforms that can provide *in vivo* biological information and thus reduce the number of animal tests, accelerating the drug discovery process [106]. Literature search on cell-based electrochemical biosensors that have been used for studying the effect of plant extracts [4,53,85], or their bioactive constituents [35,61,74,100] on mammalian cells, reveals only a fair number of reports. Based on the recent revitalization of interest in drug discovery from natural sources [7], the developments on biomaterials for biosensing applications [72,101] and the need to apply high throughput screening technologies in bioactivity detection of plant extracts [45], biosensing approaches are projected to increase.

In this study, a conducting polymer bioelectrochemical assembly was established for *in vitro* mammalian cytotoxicity/cytoprotection assessment, employing renal cell monolayers as the primary transducers for signal generation and biological sensing. Motivated by pharmacological interest in bioactive natural product-related assays, our aim was to develop an electrochemical cell-based approach that could provide cell type specific insight on the biological activity of crude drugs or their bioactive constituents.

Since PEDOTs biocompatibility has been proven with numerous cell lines, the objective of this study was to explore PEDOTs compatibility with kidney fibroblasts and fabricate an electrochemical biosensor platform able to reflect the renal cell homeostasis. For this purpose, we investigated cell adhesion, proliferation and viability indicators on kidney cells cultured on PEDOT electrode surfaces, along with the assessment of the electrodes' electrochemical state using their post-cell adhesion areal capacitance as a figure of merit for cell monolayer structural/functional status. Furthermore, the model renotoxic agent carbon tetrachloride and the widely studied medicinal plant *Salvia officinalis*, were used for the functional evaluation of the proposed assembly as a renotoxicity and renoprotection assay. To the best of our best knowledge, this is the first study describing a bioelectrochemical tool that incorporates mammalian cells, namely a cell based biosensor, with a conducting polymer for voltammetrically assaying the bioactivity of a medicinal plant extract.

2. Experimental

2.1. Materials and reagents

Dulbecco's Modified Eagle medium (DMEM), phenol red-free DMEM, L-glutamine, penicillin-streptomycin antibiotic mixture, 0.25% trypsin-EDTA solution and sodium pyruvate were purchased from Biochrom AG (Berlin, Germany). Fetal bovine serum (FBS) and Propidium iodide (PI) were purchased from Invitrogen (Massachusetts, USA). Ethidium bromide was obtained from Thermo Fisher Scientific (ACROS Organics™ brand) (Waltham, MA, USA). Carbon tetrachloride (CCl_4, PubChem CID: 5943) Neutral Red (NR), MTT (3-(4,5-dimethylthiazol-2-yl)-2,5-diphenyltetrazolium bromide), Acridine Qrange (AO), calf thymus DNA and all other reagents, unless otherwise specified, were purchased form Sigma-Aldrich (St. Louis, MO, USA). All aqueous solutions were prepared with distilled water.

2.2. Cell culture

Vero cells (continuous African green monkey kidney cell line/*Cercopithecus aethiops*/ATCC CCL-81, originally provided from LGC Promochem (Teddington, UK) were cultured in Dulbecco's Modified Eagle's Medium (DMEM) supplemented with 10% FBS, 1% L-glutamine, 100 units/ml penicillin and 100 μg/ml streptomycin, under standard cell culture conditions (5% CO_2, 95% humidity, 37 °C). Cells were maintained routinely in 75cm^2 cell culture flasks, media were replenished with fresh medium every other day and cells were subcloned through trypsinization (0.25% trypsin, 0.02% EDTA) upon 80%–90% confluency. Cell numbers were determined by hemocytometer.

2.3. Electrode sterilization and cell seeding

PEDOT screen-printed electrodes (SPEs) from Dropsens® (Llanera, Spain) (DRP-P10) were sterilized with 70% ethanol (EtOH) in phosphate buffered saline (PBS) for a few seconds and then washed three times with sterile PBS. A sanitized polystyrene cylinder tube (6 mm height, 4 mm inner diameter) was placed on top of the PEDOT working electrode, forming a cell culture microwell that can hold up to 60 μl of culture medium and defining the cell growth surface. The resulting effective seeding surface area of each electrode was 0.126 cm^2. A schematic representation of the culture setup can be seen in Fig. 1A. Prior to cell seeding, each PEDOT electrode was hydrated in DMEM for 1 h under standard cell culture conditions (5% CO_2, 95% humidity, 37 °C) to saturate the surface with growth medium and improve cell attachment.

For electrode seeding, hydration medium was replaced with 50 μl cell suspension of Vero fibroblasts (passages 129 to 135), adjusted to desired concentrations with DMEM. The cells were seeded at successive densities from 1×10^4/cm^2 to 12×10^4/cm^2 and were allowed to attach (3 h) and proliferate (24 h) under standard cell culture conditions (DMEM/10% FBS, 5% CO_2, 95% humidity, 37 °C), before further analysis. The cell monolayers on the PEDOT electrodes were regularly inspected under phase contrast microscopy, with an inverted microscope equipped with phase contrast illumination (A. Krüss - MBL3200). Electrodes from the designated time points or exposure parameters were randomly selected and harvested aseptically for performing the biochemical and electrochemical measurements.

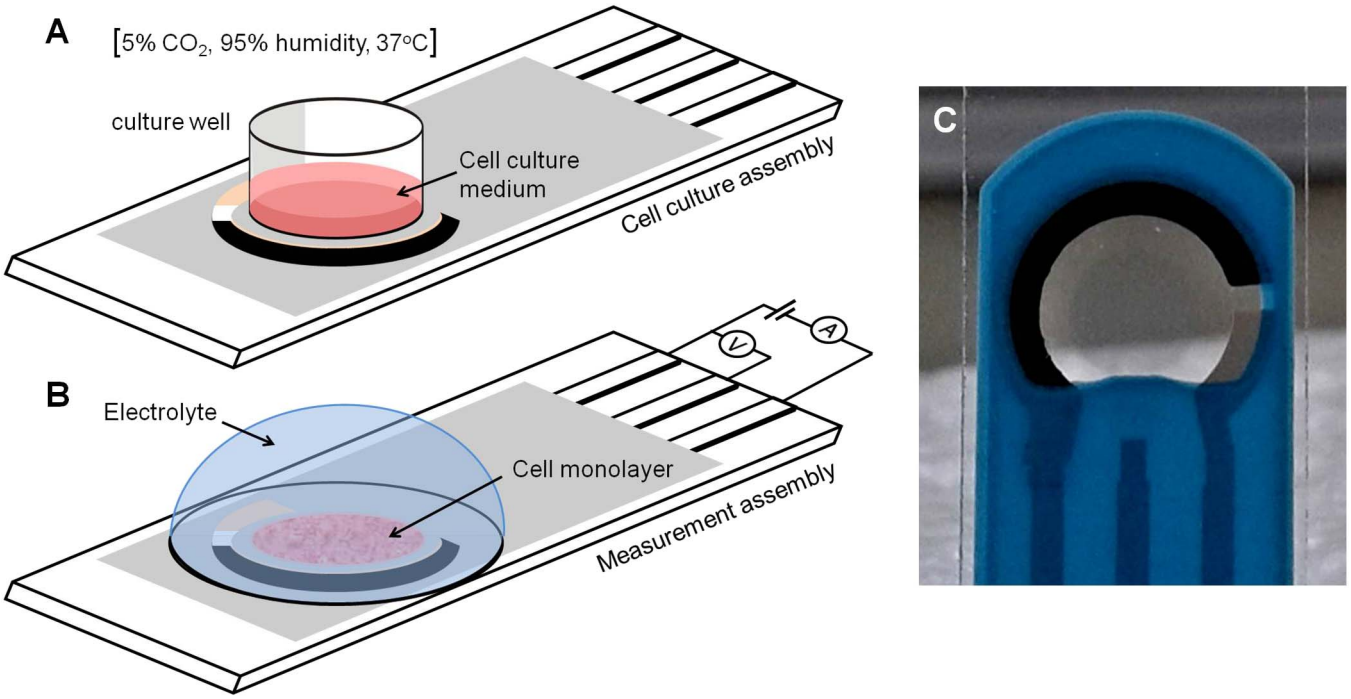

Fig. 1. Schematic representation of the culture and measurement setup. Renal cell culture assembly (A), comprising of the 3-electrode screen printed electrochemical array and a polystyrene cylinder tube placed on top of the transparent conductive polymer working electrode (C). Measurement assembly (B) of the cell-cultured electrode after culture medium aspiration with the supporting electrolyte deposited onto the array covering the three electrodes area.

2.4. DNA content assay

Cell adhesion and proliferation after 3 h and 24 h of culture were evaluated through total DNA content of the PEDOT electrodes. For the assay, the fluorophore ethidium bromide was used according to protocols previously described [15,86], with modifications. Briefly, electrodes were rinsed three times with PBS and collected in 1.5 ml eppendorf tubes and stored at − 80 °C. Frozen PEDOT electrodes were cut off from the rest of the SPE, underwent three cycles of freezing/thawing and lysed in 100 μl 0.2% (v/v) Triton X-100 and 5 mM $MgCl_2$ for 30 min to release the DNA into the solution. After centrifugation at 12,000 rpm for 10 min at 4 °C, the supernatants were collected for DNA evaluation. Subsequently, 2ul of EtBr dye working solution (5 μg/ml EtBr in 10 mM Tris base, 0.2 M NaCl, 1 mM EDTA, pH 7.4) were combined with the supernatant, transferred to clear-bottom black 96-well microtiter plates and immediately measured on a Tecan Infinite M200 Pro instrument (Tecan Group Ltd., Männedorf, Switzerland), using excitation and emission wavelengths of λ_{ex} = 546 nm and λ_{em} = 590 nm, respectively. Results were extrapolated from a standard curve using calf thymus DNA (0–20 μg/ml in 10 mM Tris-HCl, pH 7.4), 5 mM NaCl, 0.1 mM EDTA) and DNA content was expressed as μg per electrode.

2.5. Cell viability

To assess cell viability on the polymer electrode surface, cells were stained using the lysosomal stability probe neutral red (NR) and the acridine orange (AO)–propidium iodide (PI) double staining. The NR staining was performed according to the protocol described by [87] and is based on the ability of viable cells to incorporate and bind the supravital dye neutral red, a weak cationic dye that readily penetrates cell membranes by nonionic passive diffusion and accumulates in lysosomes where it binds to anionic sites in the lysosomal matrix. Briefly, at the end of the PEDOT electrode culture period (24 h), culture medium was aspirated and replaced with 50 μl NR solution (40 μg/ml NR in DMEM), followed by a 3 h incubation (37 °C, 5% CO_2, 95% humidity). At the end of incubation period, the cell monolayers on the PEODT electrodes were inspected with an inverted microscope for morphological evaluation of neutral red uptake.

For the AO/PI double staining, cells seeded on PEDOT electrodes were simultaneously stained with AO (4 μg/ml) and PI (4 μg/ml) dissolved in aqueous solution. Within 10 min, the cells were examined by fluorescence microscopy (Olympus BX40 microscope equipped with the Fluorescence Filter Cube U-MSWB) and photographed using a DP71 Olympus 12.5Mp digital camera. PI is a fluorescence dye (emission 605 nm, red), impermeable to cells with an intact plasma membrane, hence when the cell integrity becomes compromised it gains access to the nucleus, where it intercalates DNA, rendering the nucleus highly fluorescent [18]. The fluorescence dye AO (emission 515 nm, green) requires an active transport to pass through the cell membrane and thus stains nucleic acids of living cells [82]. Application of the two dyes allows visualization of both viable and nonviable cells.

2.6. Metabolic activity

Mitochondrial function of the PEDOT seeded cells was assessed through MTT assay [75]. The yellow, water soluble 3-(4,5-dimethylthiazol-2-yl)-2,5-diphenyltetrazolium bromide (MTT), can be reduced to a blue colored water-insoluble formazan by cellular mitochondrial dehydrogenases only in metabolically active cells. Briefly, at the end of the PEDOT electrode culture period (24 h), culture medium was aspirated and replaced with 50 μl MTT solution (0.5 mg/ml MTT in DMEM) followed by a 3 h incubation (37 °C, 5% CO_2, 95% humidity). At the end of incubation period, the supernatants were removed and 50 μl of DMSO was added to solubilize the crystals on top of the electrode. After standing for 10 min at room temperature, aliquots of the dissolved formazan solution were aspirated from the electrode/well assembly and added to 96-well plates. The plates were transferred to a microplate reader (BioTek™ PowerWave™ Microplate Spectrophotometer 340, Winooski, Vermont) and metabolic activity was determined by measuring optical absorbance at 570 nm *via* software (BioTek Gen5™). DMEM hydrated cell-free electrodes served as blank

control.

2.7. Nephrotoxin and plant extract exposure

After subcloning, cells were counted and transferred on polystyrene 96-well plates for viability assays (MTT) and on PEDOT microwells for electrochemical experiments. Detailed methods on plant material preparation, extraction and GC–MS/ HPLC-DAD procedures for phytochemical characterization can be found in Supplementary Information (Supplementary Methods). The concentration of plant extract used for cytoprotection experiments (7.5% v/v in DMEM) was based on MTT viability results of Vero renal cells exposed to various extract concentrations (Fig. S1). The maximum tested non-lethal dose of the aqueous extract was selected for protection against CCl_4.

2.8. Electrochemical measurements

Cyclic voltammetry (CV) experiments were performed using a computer-controlled multi-channel potentiostat PG580RM (Uniscan Instruments Ltd., Buxton, Derbyshire, UK). Electrochemical measurements were carried out using PEDOT SPEs (DRP-P10), consisting of a PEDOT working electrode (diameter 4 mm) (Fig. 1C), a carbon auxiliary electrode and a quasi-reference silver electrode on plastic substrate, with overall dimensions of L33 × W10 × H0.5 mm (Fig. 1C). Prior to running each electrochemical experiment, an SPE (Vero fibroblast-cultured or cell-free) was connected to the potentiostat through a serial port interface, the culture medium was aspirated, the PEDOT electrode was gently washed with PBS and the polystyrene tube was removed. PBS solution (0.1 M pH 7.0) was employed as supporting electrolyte. Approximately 60ul of PBS were deposited onto the SPE covering the three electrodes area (Fig. 2B) and CVs were recorded at a scan rate of 100 mV s^{-1}, in the potential range of − 1 V to + 1 V, for 1 or 10 cycles. All experiments were carried out at ambient temperature of about 25 °C.

2.9. Electrochemical analysis

Signal acquisition was realized using UiEChem™ v.1.34 software (Bio-Logic Science Instruments SAS, Claix, France). The electrode's areal capacitance C_α, on the basis of CV curves area, was calculated using the following Eq. (1):

$$C_\alpha = (2\int idV)\Big/(S(\Delta V)\nu) \quad (1)$$

where C_α is the areal capacitance (F cm^{-2}); $\int i\,dV$ (A V) is the integrated area of the CV curve; S (cm^2) is the area of the active material; ΔV (V) stands for the potential window; and ν (V s^{-1}) is the scan rate [103]. The area of the active material was calculated using the following Eq. (2):

$$S = \pi r^2{}_{PEDOT} \quad (2)$$

where S is the area of the PEDOT electrode (cm^2), π (pi) is the constant 3.14 and r is the radius of the circular electrode (cm).

2.10. Statistical analysis

All results are expressed as the mean ± SEM. Differences between means were tested for statistical significance using a one-way analysis of variance (ANOVA), followed by Tukey's post-hoc test. All statistical analyses were carried out with the SPSS Statistics v.20 (IBM Corp., Armonk, NY, USA) except dose response sigmoidal fitting which was performed with GraphPad Prism 7 (GraphPad Software, San Diego, California, USA). Unless stated otherwise, data were collected from at least three independent experiments. The level of probability for statistical significance was established at $p \leq 0.05$ for all analyses.

3. Results and discussion

3.1. PEDOT electrode's biocompatibility

In order to evaluate the efficacy of the polymer surface as substrate for cell growth and survival applications, PEDOT biocompatibility was assessed based on the parameters of cell viability, attachment, and proliferation. The renal cell culture assembly, comprising of the 3-electrode screen printed electrochemical array and a polystyrene microwell placed on top of the PEDOT working electrode surface, is schematically presented in Fig. 1A. Macroscopic images of a PEDOT screen-printed electrode and the sanitized polystyrene cylinder tube top of the working electrode surface are shown in Fig. 2A and B, while surface coverage is presented in Fig. 2C and D. Due to the polymer's transparent nature, direct visualization and viability staining of the monolayers formed by renal cells on the PEDOT surface was feasible. Inspection under phase contrast light microscopy showed normal adhesion and confluent monolayer formation (Fig. 2E, F). Cells displayed no signals of cytotoxicity, exhibiting typical plump spindle shaped fibroblast-like morphology (Fig. 2G, H), with many sites of anchorage and no types of morphological modifications, such as rounding up and detaching from the substrate, cell aggregation, or cell lysis. Furthermore, some cells adopted an elongated shape (Fig. 2G), suggesting areas of collagen formation [84].

Fig. 2I, J and K, L show the 24 h post-seeding polymer electrode surface, after applying the viability probe neutral red (NR) and after performing acridine orange (AO) - propidium iodide (PI) double staining. The NR uptake is one of the most used cytotoxicity tests with many biomedical applications [87] and is based on the ability of viable cells to incorporate and bind the supravital dye neutral red. From the microscopic observations of NR uptake by the PEDOT seeded renal fibroblast cells, it could be observed that the NR is retained in the fibroblast lysosomes and, as a result, the cells appear red (Fig. 2I, J). The uptake of neutral red derives from the ability of healthy cells to maintain pH gradients, through regular ATP production. At physiological pH, the dye's neutral net charge enables it to penetrate the cell and since the proton gradient across the lysosomal membranes, keeps the pH lower than that of the cytoplasm, the dye becomes charged and retained inside the lysosomes of undamaged cells [87]. From the fluorescence signals of AO - PI double staining, it could be observed that cells adhered and remained viable, 24 h after seeding (Fig. 2K, L). AO and PI are intercalating nucleic acid-specific fluorochromes, which emit fluorescence, when bound to DNA. AO can cross the plasma membrane of viable cells and emits green fluorescence, while PI penetrates only non-intact cells and emits red fluorescence [18]. As shown in Fig. 2K and L, the majority of the cells were stained green, maintaining normal appearance of intact cells, while only a few appeared dead, depicted in the images in red fluorescence (white arrow). Distribution of the cells after the removal of the cylinder tube which was visualized with fluorescence (Fig. M) and optical (Fig. 2N) microscopy, revealed cell monolayers confined only inside the curved walls of the culture well. The results of all the above microscopic viability assessment approaches suggest good biocompatibility of the PEDOT polymer surface with the renal cells.

3.2. Cell proliferation

To further investigate the biocompatibility of the polymer surface, quantitative results of cell proliferation of the seeded renal cells were obtained through MTT and total DNA assays. The absorbance values from the MTT assay (Fig. 2O) revealed tetrazolium reduction, suggesting metabolically active mitochondria in seeded cells. The observed time-dependent and significant increase in MTT formazan formation, between 3 h and 24 h after seeding, indicated that cells did not only adhere on the surface of the polymer electrode but also proliferated. DNA content on the electrodes was also used as a indication of renal cell

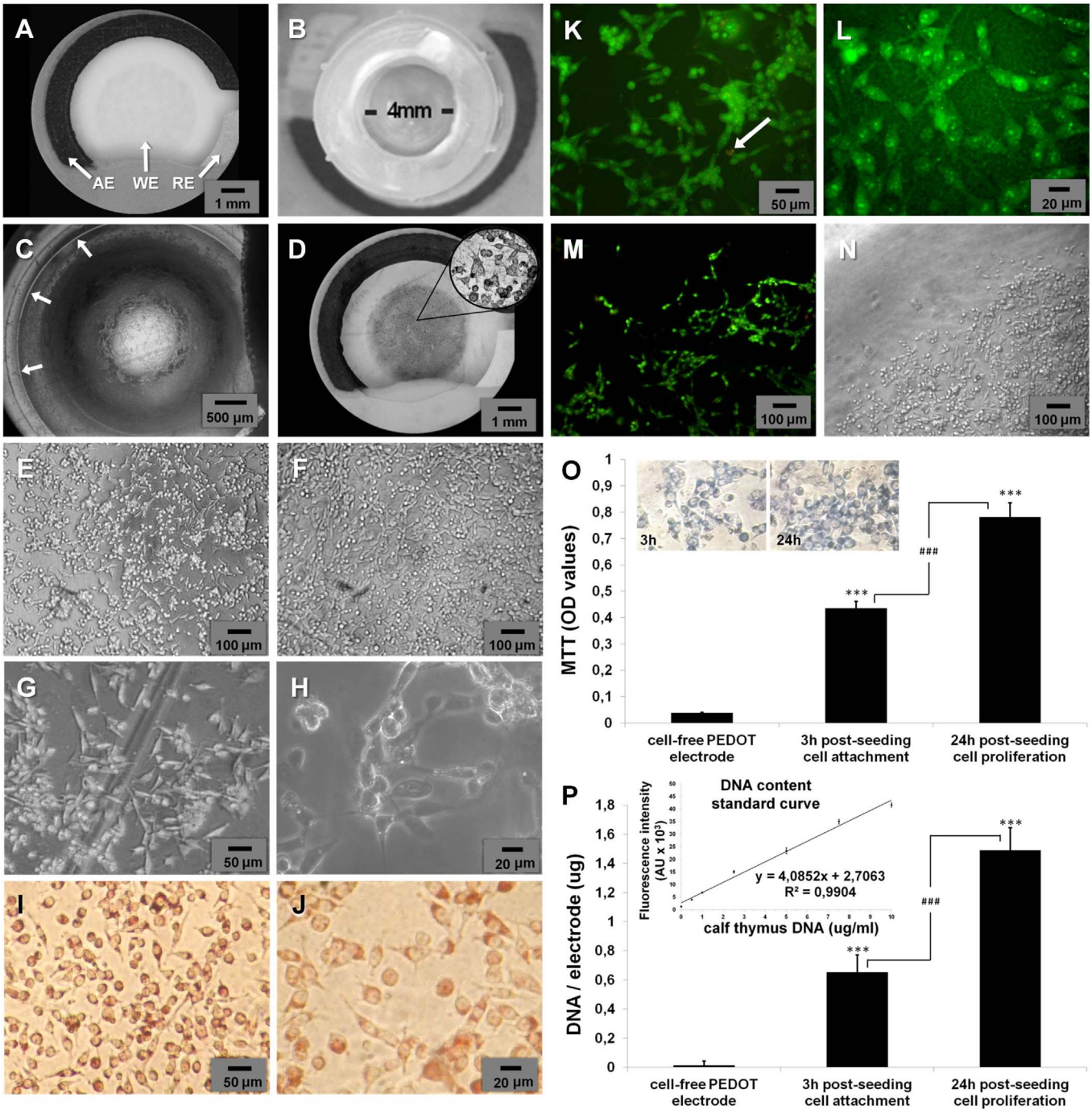

Fig. 2. Renal cell behavior on the PEDOT polymer electrode. Overview pictures of a PEDOT screen-printed electrode (A) and the sanitized polystyrene cylinder tube on top of the working electrode surface forming a microwell (B). Cellular monolayer confined along the curved walls of the culture well (C), white arrows indicate the outmost edges of the well. Cell surface coverage on Coomassie-stained PEDOT electrode at 24 h (D). Dark color indicates the presence of cells. Inlet: Coomassie-stained cells at 24 h. Phase contrast micrographs of renal fibroblast cells on the polymer electrode surface at 3 h (E) and 24 h (F, G, H) post seeding. Optical microscopy images of electrode cultured cells stained with Neutral Red (I, J). Fluorescent micrographs of acridine orange and propidium iodide double-stained renal cells cultured on the electrode polymer surface (K, L, white arrow: dead cell). Distribution of the cells at the edge of the well after the removal of the cylinder tube (M, N). Qualitative analysis of cell adhesion and proliferation measured by MTT assay (O) and DNA content (P), 3 h (cell attachment) and 24 h (cell proliferation) after seeding Vero renal fibroblasts on PEDOT electrodes. MTT values represent the optical density of the solubilized purple formazan crystals, inlet: MTT formazan accumulation inside metabolically active renal cells (i) 3 h and (ii) 24 h post seeding. DNA was determined fluorometrically through intercalation of EtBr. Fluorescence intensity units obtained from samples were extrapolated against a DNA standard curve (inlet) to determine the DNA amount per electrode. Values are expressed as mean ± standard deviation of three independent experiments, one-way ANOVA, Tukey's test, $^{***}p \leq 0.001$ vs. cell-free PEDOT and $^{\#\#\#}p \leq 0.001$ between time points.

attachment and proliferation, at 3 h and 24 h after seeding, respectively (Fig. 2P). DNA content of the cell seeded electrodes was significantly higher than the cell-free electrodes (no DNA detected) at both time points. Renal fibroblasts total DNA content increased significantly from 0.65 µg calf thymus DNA equivalents per electrode (3 h post-seeding) to 1.49 µg calf thymus DNA equivalents per electrode (24 h post-seeding) (Fig. 2P), indicating cell proliferation. Furthermore, the 24 h to 3 h post-seeding ratios of MTT absorbance and DNA content were found to be 1.79 and 2.28, respectively, close to the 24 h doubling time of actively growing Vero cells on standard tissue culture plates [77].

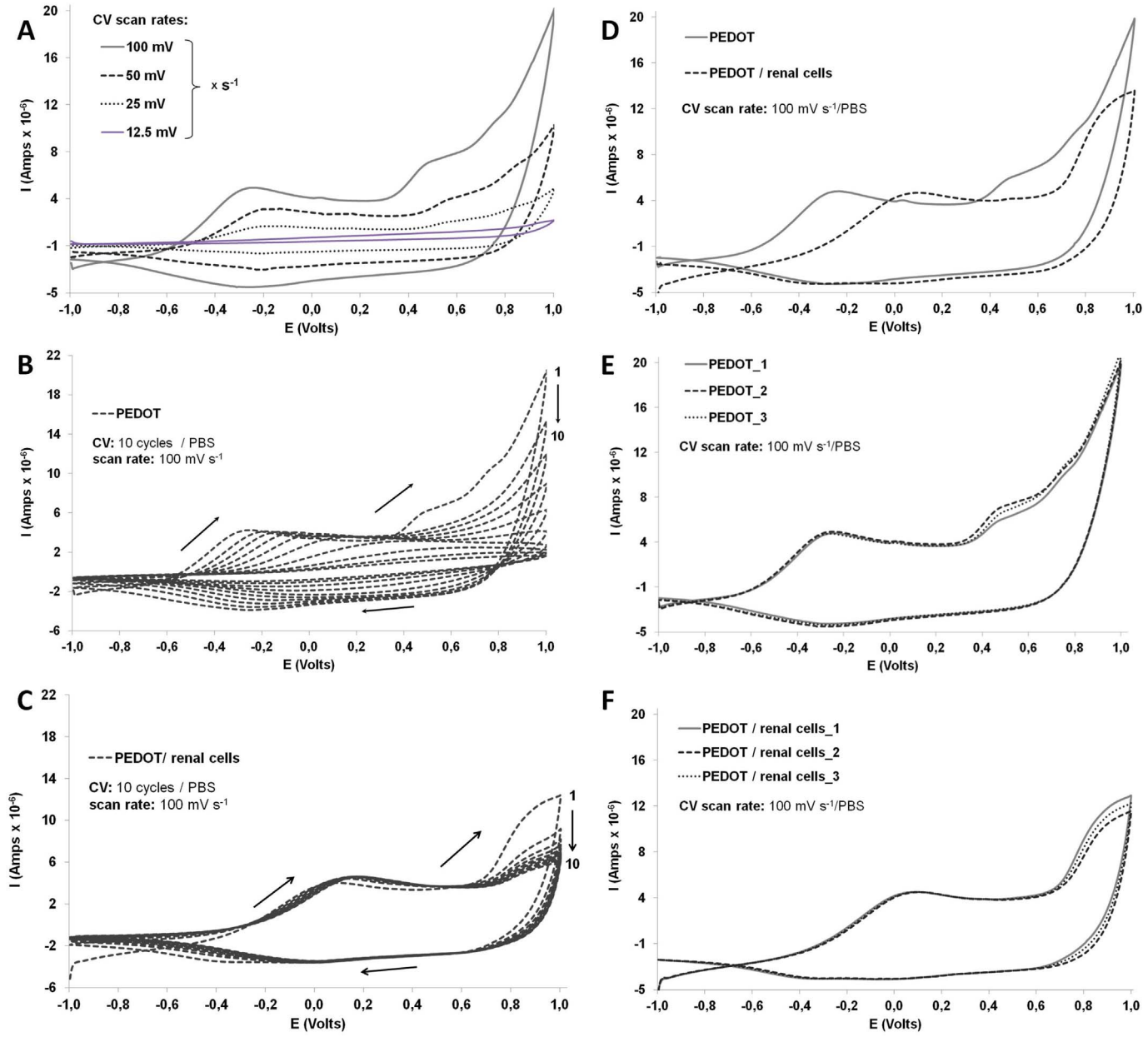

Fig. 3. Cyclic voltammograms of the conductive PEDOT polymer electrodes in PBS solution at various scans rates (A). Multiple cyclic voltammetric scans of bare (B) and cell adherent PEDOT electrodes (C) over a potential range between − 1.0 and 1.0 V with PBS as the supporting electrolyte. Cyclic voltammograms of the first scan for the bare *versus* the cell seeded PEDOT electrodes (D). Repeatability of CV profiles from three replicate scans obtained for bare (E) and renal cell cultured PEDOT electrodes (F).

3.3. Electrode characterization

The electrochemical behavior of the polymeric electrode surface was investigated using cyclic voltammetry. The anodic potential was limited to + 1 V in order to avoid the degradation of the polymer due to oxidation, as PEDOT CVs have been reported to be stable up to + 1 V, beyond which oxidation of the electrolytic medium for the polypyrroles becomes important [29,39]. Exploratory CVs performed at different scan rates, ranging from 12.5 mV s^{-1} to 100 mV s^{-1}, revealed a scan rate dependence of the anodic and cathodic peak currents as shown in Fig. 3A. Peak potentials also increased with the applied scan rate, suggesting a quasi-reversible process, where the electron transfer is comparable to the mass transport rate [19]. PEDOT exhibited a broad oxidation wave, which started at − 0.55 V and centered at about − 0.30 V, followed by a more distinguishable oxidation shoulder at + 0.29 V. This broad oxidation wave is typical of PEDOT, which, among the common conducting polymers, displays the least pronounced oxidation and reduction peaks in cyclic voltammetry and simple aqueous electrolytes, as its reduction and oxidation change is almost evenly distributed over a wide potential range [104]. A similar quasi-reversible signal, at a potential close to − 0.30 V, corresponding to the redox activity of the PEDOT polymer, has been previously reported [92]. A not so discernible reduction shoulder can be also seen around − 0.30 V, a possible reduction counterpart of the anodic wave at the same potential (Fig. 3A). In total, current peaks appeared more distinct at 100 mV s^{-1} scan rate, which was employed for all subsequent investigations.

The cycling stability of the polymeric electrode was studied by cycling the potential between − 1 V and 1 V for 10 cycles in PBS. Oxidation current densities were lower and roughly coincidental with the number of successive potential cycles, as shown in Fig. 3B, denoting the irreversibility of the process or the passivation of the polymer film due to degradation reactions from the potential scanning to relatively high anodic potentials. Furthermore, during potential cycling, the

electrode material is reduced and oxidized, leading to conformational changes of the polymer chain as well as continuous association and dissociation of dopants with the polymer matrix [78]. Both the above mentioned processes may contribute to cracking and partial delamination of the polymer film from the underlying material. Additionally, the oxidation peak at + 0.29 V disappeared completely after the first cyclic potential sweep, indicating that the oxidation process occurred mostly during the first potential cycle, or the possible formation of surface blocking species during the first scan owing to the degradation reaction described above. Therefore, the first cyclic scan was selected for all consecutive experimentations.

3.4. Electrochemical response of electrode-cultured renal cells

Cyclic voltammetry was also employed for estimating the electrocatalytic activity of the renal cell/electrode interface. As it can be shown in Fig. 3D the cell monolayer, formed through the attachment of the adherent renal cell line on the electrode surface, moved the main oxidation wave of bare PEDOT to more positive potentials, while completely hindered the oxidation shoulder around + 0.29 V and decreased the overall anodic current intensities. Additionally, a distinct oxidation shoulder appeared around + 0.9 V (Fig. 3D). These changes could the attributed to the cellular occupancy, which would result a less accessible PEDOT matrix due to the formation of an insulating layer, responsible for the bio-fouling of the film surface. Successive cyclic potential sweeps of the renal seeded electrodes showed higher stability than the bare ones. The repetitive flow of ions during cycling could result in the physical swelling and shrinking of the electrode material's lattice, the collapse of ion flow channels and the weakening the mechanisms for conducting and storing charge. The cell layer on the polymer surface might act as a physical buffer, which provides mechanical support and suppresses structural deformation during cycling.

Successive cyclic potential sweeps decreased the oxidation current intensities at + 0.9 V (Fig. 3C). Similar observations, reported previously [22,61], suggested that the decrease of anodic currents and the positive shift of peak potential could also have resulted from the possible damage inflicted to the living cells by the first voltammetric scan. Thus, the voltammetric study of the first scan was adopted for further experimentations. Data regarding the reproducibility of the cell/electrode assembly are presented in Fig. 3E, F. The recorded CVs illustrate the current responses of three individual (bare and cell-cultured) electrodes under the above mentioned electrochemical parameters. The relative standard deviations for the three independent cyclic sweeps, under the same measurement conditions, were 0.3% for the bare, and 1.2%, for the cell-seeded electrodes, respectively.

3.5. Effect of cell seeding density on the electrode capacitance

In order to investigate the influence of the number of seeded cells on the electrochemical responses of the cell-cultured polymeric electrodes, CVs of successively increasing adherent cell populations, were recorded. As shown in Fig. 4A, the overall current intensities were inversely related to cell seeding density as both anodic and cathodic current values decreased with increasing cell numbers. These changes in ionic currents were also transcribed to linearly declining capacitances of the electrodes, exhibiting a negative linear correlation (R^2 = 0.9561) as shown in Fig. 4B.

Conducting polymers, including PEDOT, are already well established as electrode materials for supercapacitors [90,95]. Their main mechanism of energy storage is based on the formation of electrical double layer (EDL) capacitance at the electrode–electrolyte interface [23,97], as well as the redox reactions. PEDOT-based supercapacitors require the diffusion of counterions in and out of the polymer (doping and dedoping) to balance the generated charges of the redox reaction [68]. This process occurs throughout the polymer film bulk due to charge exchange with the electrolyte solution in contact with the film, known as the electric capacitance of the material, or the so called redox capacitance [32]. Synergistic effects are probable with the combination of the capacitive charging of the EDL and a redox reaction in a way that both charge storage mechanisms work in parallel, with the overall capacitance of the composite electrode being the sum of the EDL capacitance and the redox capacity [59].

The electrochemical performance of polymers as supercapacitors can be measured either by two-electrode or three-electrode configurations [107]. The present electrochemical assembly utilizes the three-electrode configuration and cyclic voltammetry (CV), one of the most commonly used methods for supercapacitor characterization [107]. Due to the low mass of the PEDOT material, the mass of the electrode cannot be accurately determined, thus we report the capacitance values as areal capacitances [66].

The proposed mechanism for the decrease in the electrode's capacitance upon the mammalian cell monolayer formation is based both on the model of the EDL that is set up at the electrode-electrolyte interface [81,97] and the redox surface reactions [59]. Different models of the EDL were stated by Helmholtz, Gouy-Chapman, Stern, or Grahame [12]. The boundary that is formed when the electronic conductor, *viz.* PEDOT, is brought in contact with the liquid ionic conductor, *viz.* electrolyte (Fig. 5C (i)), is the region that behaves like a capacitor [58]. The presence of a biological layer at the surface of the electrode, after cell adhesion and proliferation, might disrupt the EDL formation, leading to capacitance regression mainly due to poor EDL behavior (Fig. 5C (iii)). The affinity between the electrode and the electrolyte is known to be crucial for supercapacitors, since double-layer charge storage is strongly dependent on the surface contact areas, which greatly influence the capacitance of the device [93]. Additionally, the formation of the cell monolayer on the electrode could also suppress the surface redox processes (Fig. 5C (ii)) by hindering the penetration of redox species deeper into the polymer films and affecting its redox capacitance (Fig. 5C (iv)). Naturally, in composite CP based electrodes, a synergistic effect between the EDL capacitance charging and the concurrent redox (pseudocapacitance) reaction occurs, with the later to contribute to the overall capacitance of the electrode [10].

3.6. Assessment of CCl_4-mediated renotoxicity and Salvia officinalis renoprotection

After establishing a correlation between cell number and electrochemical responses, the renotoxicity agent CCl_4 and the widely studied medicinal plant *Salvia officinalis* were selected as models to assess the ability of the proposed assembly to monitor renal cell homeostasis. CCl_4 produces acute renal injury in a number of mammalian species [40] and has been extensively used as a model compound to induce hepatotoxicity and nephrotoxicity both *in vivo* [1,34,46,51,52] and *in vitro* [80,49]. *Salvia officinalis* L. (Lamiaceae), commonly known as sage, is an aromatic and medicinal plant which has been used for millennia for its beneficial effects in the prevention and treatment of various pathological disorders [13]. In Latin, *Salvia* means “to cure”, while *officinalis*, means “medicinal” [37]. Among their numerous healing properties, sage extracts have been widely studied with respect to their hepatoprotective [3,48,55,64] and nephroprotective [27,62,71] effects. All the cytoprotection tests were carried out with a non-cytotoxic concentration of the extract, since we were interested in potent protective activity without deleterious effects on the cells. Concentrations up to 7.5% aqueous plant extract showed no cytotoxicity based on the MTT assay (Fig. S1), while 15% plant extract showed decreased viability to approximately 30%. This loss of viability can be attributed to changes in osmotic pressure due to the large amount of crude plant extract in the cell culture medium.

To study effect of CCl_4 on the capacitance of the renal cell cultured electrodes, cells were allowed to attach themselves on the electrode surface (3 h, $6 \times 10^4/cm^2$) before treatment with different concentrations of the nephrotoxin for 24 h. At the end of the exposure period, the

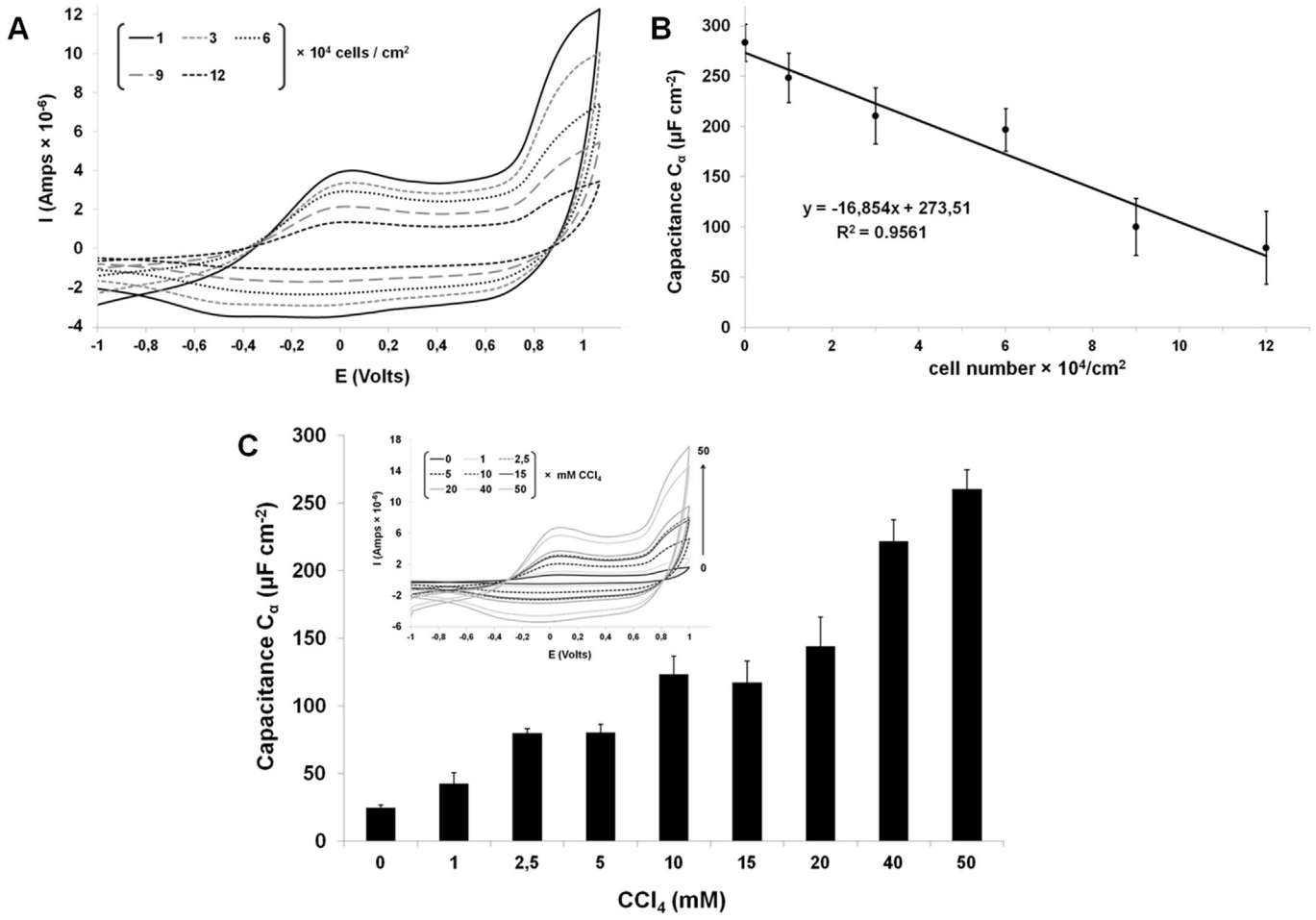

Fig. 4. Cyclic voltammetric scan responses of the presented assembly to various cell seeding densities (A). Relationship between cell density and adherent electrode capacitances (B). Variations on capacitances caused by CCl_4 exposure to renal cell adherent electrodes (C), (inlet: respective CVs). Values are expressed as mean ± SEM of three independent experiments.

toxin-containing culture medium was aspirated, the electrodes were gently washed with PBS and CVs were recorded as described above, with their respective capacitances plotted against CCl_4 doses, as shown in Fig. 4C. CCl_4 24 h exposure resulted in a dose-dependent increase in the CVs ionic currents and consecutively the electrode's capacitance.

To examine whether the observed increase in capacitance is correlated with the effects of the nephrotoxin in cell viability and provide a comparison with a standard quantitative cytotoxicity assessment method, CCl_4 exposed cells were assayed for changes in their cellular metabolic activity by the MTT reduction assay, which assesses cytotoxicity in the form of mitochondrial dehydrogenase activity [75]. CCl_4 showed significant cytotoxic effects against renal cells, after 24 h incubation, with a maximal cytotoxic effect observed at concentrations over 40 mM. Fitting with a dose response curve (Fig. 5A) indicated a median lethal concentration, LC_{50}, of 6.06 mM. Similar to the renal viability data obtained in this study, previous studies on mammalian cells have reported maximal cytotoxic effects at 40 mM after CCl_4 exposure [21], while others [63] showed a decreased survival rate of HepG2 hepatocytes to 32%, after 24 h exposure to 10 mM CCl_4, comparable with the presented renal cytotoxicity results.

The cytotoxic effect of the CCl_4 was indicated by a decrease in MTT values and an increase in electrode's capacitance. For dose-response dependent cytotoxicity comparison, capacitance values were normalized at 100% for the highest response (50 mM CCl_4 treatment) and fitted to a sigmoidal curve (Fig. 5B), providing a half maximal effective concentration, EC_{50}, of 5.85 mM. The difference between the two values could be associated with the different principles for estimating viability and with CCl_4 mode of action. The proposed biosensor detects not only cell number but cell adhesion, spreading and monolayer formation, while MTT assesses cytotoxicity in the form of reduced cell viability through the reduction of mitochondrial dehydrogenase activity, indirectly measuring cell metabolism [99]. CCl_4 is a drastic organic nephrotoxin [105]. Its cytotoxic mechanism is postulated to result from the free radicals released during its metabolism [73]. These highly reactive primary metabolites, trichloromethyl and trichloromethyl peroxy free radicals, are capable of covalently binding to cellular macromolecules and initiating lipid peroxidation by attacking polyunsaturated fatty acids in membranes, causing membrane disruption and consecutive cell death [73]. During the death process, cells display loss of anchorage, they become permeable and eventually undergo complete fragmentation [56]. Since the CCl_4 exposed cell monolayers are obliterated, leading to electrode surfaces devoid of cells, the electrode-electrolyte interface is liberated, resulting stronger EDL behavior, unobstructed redox reactions and elevated capacitance (Fig. 5C, D). Other investigators have reported similar observations with increased capacitance of fibroblast cultured polymers upon cell detachment after the addition of adhesion perturbing agents such as trypsin [65].

Salvia officinalis cytoprotection was demonstrated by both the MTT and the proposed biosensor assay. Many studies associate *S. officinalis* bioactive properties to its polyphenol content [69]. Leaves of sage are well known for their phenolic structure-based antioxidative potency [13]. The most abundant phenolic compounds found in the extract were rosmarinic acid isomers and derivatives (Table S2), which according to literature exhibit very high superoxide scavenging activities and are more likely to be responsible for most of sage's antioxidant properties [69]. Luteolin glycuronide, a flavonoid commonly found in *Salvia*

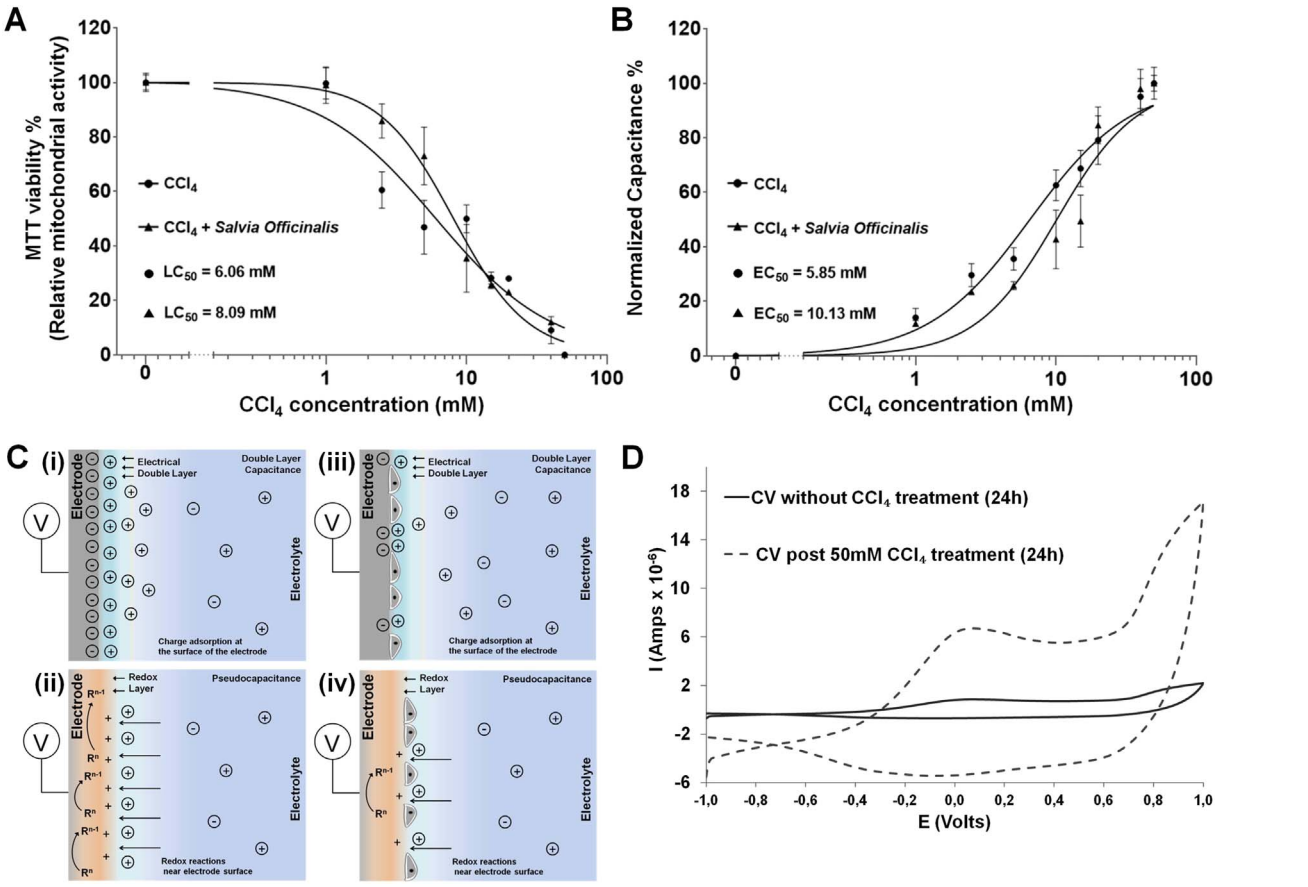

Fig. 5. Dose-response curves for renal CCl_4 exposure (black circles) and for CCl_4 - *Salvia officinalis* co-exposure (black triangles), on the inhibition of cell viability (A) and normalized capacitance (B) fitted by non-linear regression. Proposed mechanism for the decrease in the electrode's capacitance upon mammalian cell monolayer formation (C). Matching CVs of cell adhered electrodes without CCl_4 treatment (undamaged cell monolayer) and CCl_4 treated electrodes with damaged and/or dead cells (D).

species, was also among the main water soluble compounds of the studied plant extract (Table S2). Luteolin has been shown to protect cells against CCl_4-induced toxicity in previous studies [28,60]. The terpenes camphor and 1,8-cineole were the main plant extract volatile compounds (Table S1). The monoterpene 1,8-cineole has been reported to attenuate hydrogen peroxide cytotoxicity [83], while camphor and 1,8-cineole have been identified as anti-inflammatory compounds of a *Salvia officinalis* infusion applied in human fibroblasts [31]. Furthermore, camphor induced fibroblast proliferation and collagen formation in dermal fibroblasts [102].

The sage extract ameliorated CCl_4-induced cytotoxicity, with its protective action indicated as increases in both LC_{50} (MTT) and EC_{50} (biosensor) values. As shown in Fig. 5A LC_{50} increased from 6.06 mM to 8.08 mM after sage extract and CCl_4 co-exposure, while EC_{50} increased from 5.85 mM to 10.13 mM. The difference between EC_{50} and LC_{50} could be associated with the different principles for estimating viability as described above. Additionally, plant extracts and polyphenolic compounds have been reported to interfere with the MTT assay and lead to false positive or false negative results [20].

4. Conclusions

In this study, a cell-based bioelectrochemical assembly that utilizes a conducting polymer was established for cytotoxicity and/or cytoprotection assessment. The biocompatible polymer electrodes provided a platform for renal cell culture and biological sensing *in vitro*. As shown by the results, the proposed system can reflect toxicity and cytoprotective function through cell monolayer formation on a biocompatible electrode surface, in agreement with the well-established MTT assay of cell viability. Application of a known medicinal plant extract and a model nephrotoxin demonstrated the feasibility of the proposed sensing assembly for effective cell specific screening of pharmacologically active substances or crude plant extracts.

Transparency document

The http://dx.doi.org/10.1016/j.bbagen.2017.06.021 associated with this article can be found, in online version.

Acknowledgments

Part of this research has been co-financed by the European Union (European Social Fund - ESF) and Greek National Funds through the Operational Program “Education and Lifelong Learning” of the National Strategic Reference Framework (NSRF) - Research Funding Program: Heracleitus II. Investing in knowledge society through the European Social Fund.

Appendix A. Supplementary data

Supplementary data to this article can be found online at http://dx.doi.org/10.1016/j.bbagen.2017.06.021.

References

[1] T.-H. Ahn, Y.-S. Yang, J.-C. Lee, C.-J. Moon, S.-H. Kim, W. Jun, S.-C. Park, J.-C. Kim, Ameliorative effects of Pycnogenol® on carbon tetrachloride-induced hepatic oxidative damage in rats, Phytother. Res. 21 (2007) 1015–1019, http://dx.doi.org/10.1002/ptr.2146.

[2] T. Ahuja, I.A. Mir, D. Kumar, Rajesh, Biomolecular immobilization on conducting polymers for biosensing applications, Biomaterials 28 (2007) 791–805, http://dx.doi.org/10.1016/j.biomaterials.2006.09.046.

[3] A. Amin, A.A. Hamza, Hepatoprotective effects of *Hibiscus*, *Rosmarinus* and *Salvia* on azathioprine-induced toxicity in rats, Life Sci. 77 (2005) 266–278, http://dx.doi.org/10.1016/j.lfs.2004.09.048.

[4] B. Antonio, G. Antonella, C. Angela, B. Gianfranco, D. 'Antuono Isabella, R. Gaia, F. Angela, L. Vito, D. 'Hallewin Guy, S.P. Andrea, M. Fiorenza, Real-time monitoring of glucose and phenols intestinal absorption through an integrated Caco-2TC7cells/biosensors telemetric device: hypoglycemic effect of fruit phytochemicals, Biosens. Bioelectron. 88 (2017) 159–166, http://dx.doi.org/10.1016/j.bios.2016.08.007.

[5] T. Arora, A.K. Mehta, V. Joshi, K.D. Mehta, N. Rathor, P.K. Mediratta, K.K. Sharma, Substitute of animals in drug research: an approach towards fulfillment of 4R's, Indian J. Pharm. Sci. 73 (2011) 1–6, http://dx.doi.org/10.4103/0250-474X.89750.

[6] M. Asplund, E. Thaning, J. Lundberg, A.C. Sandberg-Nordqvist, B. Kostyszyn, O. Inganäs, H. von Holst, Toxicity evaluation of PEDOT/biomolecular composites intended for neural communication electrodes, Biomed. Mater. 4 (2009) 45009, http://dx.doi.org/10.1088/1748-6041/4/4/045009.

[7] A.G. Atanasov, B. Waltenberger, E.-M. Pferschy-Wenzig, T. Linder, C. Wawrosch, P. Uhrin, V. Temml, L. Wang, S. Schwaiger, E.H. Heiss, J.M. Rollinger, D. Schuster, J.M. Breuss, V. Bochkov, M.D. Mihovilovic, B. Kopp, R. Bauer, V.M. Dirsch, H. Stuppner, Discovery and resupply of pharmacologically active plant-derived natural products: a review, Biotechnol. Adv. 33 (2015) 1582–1614, http://dx.doi.org/10.1016/j.biotechadv.2015.08.001.

[8] M. Ates, A review study of (bio)sensor systems based on conducting polymers, Mater. Sci. Eng. C 33 (2013) 1853–1859, http://dx.doi.org/10.1016/j.msec.2013.01.035.

[9] N. Aydemir, J. Malmström, J. Travas-Sejdic, Conducting polymer based electrochemical biosensors, Phys. Chem. Chem. Phys. 18 (2016) 8264–8277, http://dx.doi.org/10.1039/c5cp06830d.

[10] V.S. Bagotsky, A.M. Skundin, Y.M. Volfkovich, Electrochemical Power Sources: Batteries, Fuel Cells, and Supercapacitors, Electrochemical Power Sources: Batteries, Fuel Cells, and Supercapacitors, (2015), http://dx.doi.org/10.1002/9781118942857.

[11] P. Banerjee, A.K. Bhunia, Mammalian cell-based biosensors for pathogens and toxins, Trends Biotechnol. (2009), http://dx.doi.org/10.1016/j.tibtech.2008.11.006.

[12] A.J. Bard, L.R. Faulkner, Electrochemical Methods: Fundamentals and Applications, Wiley, 2001.

[13] D. Baricevic, T. Bartol, V. Pharmacology 11. The biological/pharmacological activity of the *Salvia* genus, in: S. Kintzios (Ed.), The Genus *Salvia*, Harwood Academic Publishers, Amsterdam, 2000, pp. 143–184.

[14] M.H. Bolin, K. Svennersten, D. Nilsson, A. Sawatdee, E.W.H. Jager, A. Richter-Dahlfors, M. Berggren, Active control of epithelial cell-density gradients grown along the channel of an organic electrochemical transistor, Adv. Mater. 21 (2009) 4379–4382, http://dx.doi.org/10.1002/adma.200901191.

[15] V. Bonasera, S. Alberti, A. Sacchetti, Protocol for high-sensitivity/long linear-range spectrofluorimetric DNA quantification using ethidium bromide, Biotechniques (2007).

[16] M. Bongo, O. Winther-Jensen, S. Himmelberger, X. Strakosas, M. Ramuz, A. Hama, E. Stavrinidou, G.G. Malliaras, A. Salleo, B. Winther-Jensen, R.M. Owens, PEDOT:gelatin composites mediate brain endothelial cell adhesion, J. Mater. Chem. B 1 (2013) 3860, http://dx.doi.org/10.1039/c3tb20374c.

[17] L. Bousse, Whole cell biosensors, Sensors Actuators B Chem. 34 (1996) 270–275, http://dx.doi.org/10.1016/S0925-4005(96)01906-5.

[18] C. Brana, C. Benham, L. Sundstrom, A method for characterising cell death in vitro by combining propidium iodide staining with immunohistochemistry, Brain Res. Brain Res. Protoc. 10 (2002) 109–114.

[19] D.A.C. Brownson, C.E. Banks, Interpreting Electrochemistry, The Handbook of Graphene Electrochemistry, Springer, London, 2014, pp. 23–77, http://dx.doi.org/10.1007/978-1-4471-6428-9_2 (London).

[20] R. Bruggisser, K. von Daeniken, G. Jundt, W. Schaffner, H. Tullberg-Reinert, Interference of plant extracts, phytoestrogens and antioxidants with the MTT Tetrazolium assay, Planta Med. 68 (2002) 445–448, http://dx.doi.org/10.1055/s-2002-32073.

[21] H.-M. Chang, Y.-W. Liao, C.-H. Chiang, Y.-J. Chen, Y.-H. Lai, Y.-L. Chang, H.-L. Chen, S.-Y. Jeng, J.-H. Hsieh, C.-H. Peng, H.-Y. Li, Y. Chien, S.-Y. Chen, L.-K. Chen, T.-I. Huo, Improvement of carbon tetrachloride-induced acute hepatic failure by transplantation of induced pluripotent stem cells without reprogramming factor c-Myc, Int. J. Mol. Sci. 13 (2012) 3598–3617, http://dx.doi.org/10.3390/ijms13033598.

[22] Y. Ci, Q. Zhai, S. Wang, W. Chang, C. Zhang, H. Ma, D. Chen, M. Zhao, S. Hu, Voltammetric studies of the effect of cisplatin-liposome on Hela cells, Talanta 55 (2001) 693–698, http://dx.doi.org/10.1016/S0039-9140(01)00480-5.

[23] B.E. Conway, W.G. Pell, T.C. Liu, Diagnostic analyses for mechanisms of self-discharge of electrochemical capacitors and batteries, J. Power Sources 65 (1997) 53–59.

[24] L.J. del Valle, F. Estrany, E. Armelin, R. Oliver, C. Alemán, Cellular adhesion, proliferation and viability on conducting polymer substrates, Macromol. Biosci. 8 (2008) 1144–1151, http://dx.doi.org/10.1002/mabi.200800101.

[25] D. Devost, N. Audet, C. Zhou, H. Kobayashi, H. Bonin, V. Lukashova, C. Le Gouill, M. Bouvier, T.E. Hébert, Chapter 15 – cellular and subcellular context determine outputs from signaling biosensors, Methods Cell Biol. 132 (2016) 319–337, http://dx.doi.org/10.1016/bs.mcb.2015.11.010.

[26] M. Dietrich, J. Heinze, G. Heywang, F. Jonas, Electrochemical and spectroscopic characterization of polyalkylenedioxythiophenes, J. Electroanal. Chem. 369 (1994) 87–92, http://dx.doi.org/10.1016/0022-0728(94)87085-3.

[27] K. Dizaye, Alleviation of Cisplatin-induced Nephrotoxicity in Albino Rats by Aqueous Extract of *Salvia officinalis*, (2015), p. 1.

[28] R. Domitrović, H. Jakovac, J. Tomac, I. Šain, Liver fibrosis in mice induced by carbon tetrachloride and its reversion by luteolin, Toxicol. Appl. Pharmacol. 241 (2009) 311–321, http://dx.doi.org/10.1016/j.taap.2009.09.001.

[29] X. Du, Z. Wang, Effects of polymerization potential on the properties of electrosynthesized PEDOT films, Electrochim. Acta 48 (2003) 1713–1717, http://dx.doi.org/10.1016/S0013-4686(03)00143-9.

[30] H. Ecken, S. Ingebrandt, M. Krause, D. Richter, M. Hara, A. Offenhäusser, 64-Channel extended gate electrode arrays for extracellular signal recording, Electrochim. Acta 48 (2003) 3355–3362, http://dx.doi.org/10.1016/S0013-4686(03)00405-5.

[31] M.M. Ehrnhöfer-Ressler, K. Fricke, M. Pignitter, J.M. Walker, J. Walker, M. Rychlik, V. Somoza, Identification of 1,8-cineole, borneol, camphor, and thujone as anti-inflammatory compounds in a *Salvia officinalis* L. infusion using human gingival fibroblasts, J. Agric. Food Chem. 61 (2013) 3451–3459, http://dx.doi.org/10.1021/jf305472t.

[32] S.N. Eliseeva, D.V. Spiridonova, E.G. Tolstopyatova, V.V. Kondratiev, Redox capacitance of poly-3,4-ethylenedioxythiophene studied by cyclic voltammetry and faradaic impedance spectroscopy, Russ. J. Electrochem. 44 (2008) 894–900, http://dx.doi.org/10.1134/S102319350808003X.

[33] A. Elschner, PEDOT: Principles and Applications of an Intrinsically Conductive Polymer, CRC Press, 2011.

[34] Z.A. Fadhel, S. Amran, Effects of black tea extract on carbon tetrachloride-induced lipid peroxidation in liver, kidneys, and testes of rats, Phytother. Res. 16 (2002) 28–32, http://dx.doi.org/10.1002/ptr.793.

[35] J. Feng, G.-A. Luo, H.-Y. Jian, R.-G. Wang, C.-C. An, Voltammetric behavior of tumor cells U937 and its usefulness in evaluating the effect of caffeic acid, Electroanalysis 12 (2000) 513–516, http://dx.doi.org/10.1002/(SICI)1521-4109(200005)12:7<513::AID-ELAN513>3.0.CO;2-D.

[36] W. Franks, S. Tosatti, F. Heer, P. Seif, M. Textor, A. Hierlemann, Patterned cell adhesion by self-assembled structures for use with a CMOS cell-based biosensor, Biosens. Bioelectron. 22 (2007) 1426–1433, http://dx.doi.org/10.1016/j.bios.2006.06.031.

[37] I. Generalić, D. Skroza, J. Šurjak, S.S. Možina, I. Ljubenkov, A. Katalinić, V. Šimat, V. Katalinić, Seasonal variations of phenolic compounds and biological properties in sage (*Salvia officinalis* L.), Chem. Biodivers. 9 (2012) 441–457, http://dx.doi.org/10.1002/cbdv.201100219.

[38] M. Gerard, A. Chaubey, B.D. Malhotra, Application of conducting polymers to biosensors, Biosens. Bioelectron. 17 (2002) 345–359, http://dx.doi.org/10.1016/S0956-5663(01)00312-8.

[39] G. Zotti, S. Zecchin, G. Schiavon, L.B. Groenendaal, Conductive and magnetic properties of 3, 4-dimethoxy-and 3, 4-ethylenedioxy-capped polypyrrole and polythiophene, Chemistry of materials 12 (10) (2000) 2996–3005.

[40] R.S. Goldstein, W.R. Hewitt, J.B. Hook, Toxic Interactions, Elsevier Science, 2013.

[41] R.A. Green, N.H. Lovell, L.A. Poole-Warren, Impact of co-incorporating laminin peptide dopants and neurotrophic growth factors on conducting polymer properties, Acta Biomater. 6 (2010) 63–71, http://dx.doi.org/10.1016/j.actbio.2009.06.030.

[42] L. Groenendaal, F. Jonas, D. Freitag, H. Pielartzik, J.R. Reynolds, Poly(3,4-ethylenedioxythiophene) and its derivatives: past, present, and future, Adv. Mater. 12 (2000) 481–494, http://dx.doi.org/10.1002/(SICI)1521-4095(200004)12:7<481::AID-ADMA481>3.0.CO;2-C.

[43] M. Guo, J. Chen, Y. Zhang, K. Chen, C. Pan, S. Yao, Enhanced adhesion/spreading and proliferation of mammalian cells on electropolymerized porphyrin film for biosensing applications, Biosens. Bioelectron. 23 (2008) 865–871, http://dx.doi.org/10.1016/j.bios.2007.09.006.

[44] M. Heinrich, Ethnopharmacology in the 21st century - grand challenges, Front. Pharmacol. 1 (2010) 8, http://dx.doi.org/10.3389/fphar.2010.00008.

[45] C.J. Henrich, J.A. Beutler, Matching the power of high throughput screening to the chemical diversity of natural products, Nat. Prod. Rep. 30 (2013) 1284, http://dx.doi.org/10.1039/c3np70052f.

[46] A.A. Hismiogullari, S.E. Hismiogullari, O. Karaca, F.B. Sunay, S. Paksoy, M. Can, I. Kus, K. Seyrek, O. Yavuz, The protective effect of curcumin administration on carbon tetrachloride (CCl4)-induced nephrotoxicity in rats, Pharmacol. Rep. 67 (2015) 410–416, http://dx.doi.org/10.1016/j.pharep.2014.10.021.

[48] Y. Jiang, L. Zhang, H.P.V. Rupasinghe, Antiproliferative effects of extracts from *Salvia officinalis* L. and *Saliva miltiorrhiza* Bunge on hepatocellular carcinoma cells, Biomed Pharmacother 85 (2017) 57–67, http://dx.doi.org/10.1016/j.biopha.2016.11.113.

[49] X. Jin, T. Cong, L. Zhao, L. Ma, R. Li, P. Zhao, C. Guo, The protective effects of Masson pine pollen aqueous extract on CCl4-induced oxidative damage of human hepatic cells, Int. J. Clin. Exp. Med. 8 (2015) 17773–17780.

[50] V. Karagkiozaki, P.G. Karagiannidis, M. Gioti, P. Kavatzikidou, D. Georgiou, E. Georgaraki, S. Logothetidis, Bioelectronics meets nanomedicine for cardiovascular implants: PEDOT-based nanocoatings for tissue regeneration, Biochim. Biophys. Acta 1830 (2013) 4294–4304, http://dx.doi.org/10.1016/j.bbagen.2012.12.019.

[51] R.A. Khan, M.R. Khan, S. Sahreen, J. Bokhari, Prevention of CCl4-induced nephrotoxicity with *Sonchus asper* in rat, Food Chem. Toxicol. 48 (2010) 2469–2476, http://dx.doi.org/10.1016/j.fct.2010.06.016.

[52] H.-Y. Kim, J.-K. Kim, J.-H. Choi, J.-Y. Jung, W.-Y. Oh, D.C. Kim, H.S. Lee, Y.S. Kim, S.S. Kang, S.-H. Lee, S.-M. Lee, Hepatoprotective effect of pinoresinol on carbon tetrachloride-induced hepatic damage in mice, J. Pharmacol. Sci. 112 (2010) 105–112.

[53] S. Kintzios, K. Papageorgiou, I. Yiakoumettis, D. Baričevič, A. Kušar, Evaluation of the antioxidants activities of four Slovene medicinal plant species by traditional and novel biosensory assays, J. Pharm. Biomed. Anal. (2010), http://dx.doi.org/10.1016/j.jpba.2010.05.013.

[54] S.E. Kintzios, Cell-based biosensors in clinical chemistry, Mini-Rev. Med. Chem. 7 (2007) 1019–1026.

[55] K. Kozics, V. Klusová, A. Srančíková, P. Mučaji, D. Slameňová, Ľ. Hunáková, B. Kusznierewicz, E. Horváthová, Effects of *Salvia officinalis* and *Thymus vulgaris* on oxidant-induced DNA damage and antioxidant status in HepG2 cells, Food Chem. 141 (2013) 2198–2206, http://dx.doi.org/10.1016/j.foodchem.2013.04.089.

[56] G. Kroemer, L. Galluzzi, P. Vandenabeele, J. Abrams, E.S. Alnemri,

E.H. Baehrecke, M.V. Blagosklonny, W.S. El-Deiry, P. Golstein, D.R. Green, M. Hengartner, R.A. Knight, S. Kumar, S.A. Lipton, W. Malorni, G. Nunez, M.E. Peter, J. Tschopp, J. Yuan, M. Piacentini, B. Zhivotovsky, G. Melino, Classification of cell death: recommendations of the Nomenclature Committee on Cell Death 2009, Cell Death Differ. 16 (2009) 3–11, http://dx.doi.org/10.1038/cdd.2008.150.

[57] G. Lanzani, Materials for bioelectronics: organic electronics meets biology, Nat. Mater. 13 (2014) 775–776, http://dx.doi.org/10.1038/nmat4021.

[58] D.W. Lee, D.J. Im, I.S. Kang, Electric double layer at the interface of ionic liquid–dielectric liquid under electric field, Langmuir 29 (2013) 1875–1884, http://dx.doi.org/10.1021/la3040775.

[59] K.W. Leitner, B. Gollas, M. Winter, J.O. Besenhard, Combination of redox capacity and double layer capacitance in composite electrodes through immobilization of an organic redox couple on carbon black, Electrochim. Acta 50 (2004) 199–204, http://dx.doi.org/10.1016/j.electacta.2004.07.030.

[60] J. Li, X. Li, W. Xu, S. Wang, Z. Hu, Q. Zhang, X. Deng, J. Wang, J. Zhang, C. Guo, Antifibrotic effects of luteolin on hepatic stellate cells and liver fibrosis by targeting AKT/mTOR/p70S6K and TGFβ/Smad signalling pathways, Liver Int. 35 (2015) 1222–1233, http://dx.doi.org/10.1111/liv.12638.

[61] J. Li, X. Liu, M. Guo, Y. Liu, S. Liu, S. Yao, Electrochemical study of breast cancer cells MCF-7 and its application in evaluating the effect of diosgenin, Anal. Sci. 21 (2005) 561–564.

[62] L. Li, Y. Zhang, J. Ma, W. Dong, Q. Song, J. Zhang, L. Chu, *Salvia miltiorrhiza* injection ameliorates renal damage induced by lead exposure in mice, Sci. World J. 2014 (2014) 1–9, http://dx.doi.org/10.1155/2014/572697.

[63] X.-W. Li, R. Zhu, B. Li, M. Zhou, Q.-J. Sheng, Y.-P. Yang, N.-Y. Han, Z.-Q. Li, Mechanism underlying carbon tetrachloride-inhibited protein synthesis in liver, World J. Gastroenterol. 16 (2010) 3950–3956, http://dx.doi.org/10.3748/wjg.v16.i31.3950.

[64] C.F. Lima, P.C.R. Valentao, P.B. Andrade, R.M. Seabra, M. Fernandes-Ferreira, C. Pereira-Wilson, Water and methanolic extracts of *Salvia officinalis* protect HepG2 cells from t-BHP induced oxidative damage, Chem. Biol. Interact. 167 (2007) 107–115, http://dx.doi.org/10.1016/j.cbi.2007.01.020.

[65] P. Lin, F. Yan, J. Yu, H.L.W. Chan, M. Yang, The application of organic electrochemical transistors in cell-based biosensors, Adv. Mater. 22 (2010) 3655–3660, http://dx.doi.org/10.1002/adma.201000971.

[66] T. Lindfors, Electrochemical Reduction of Graphene Oxide in Electrically Conducting Poly(3,4-Ethylenedioxythiophene) Films 110, (2013), pp. 428–436, http://dx.doi.org/10.1016/J.ELECTRACTA.2013.03.070.

[67] Q. Liu, C. Wu, H. Cai, N. Hu, J. Zhou, P. Wang, Cell-based biosensors and their application in biomedicine, Chem. Rev. 114 (2014) 6423–6461, http://dx.doi.org/10.1021/cr2003129.

[68] R. Liu, S. Il Cho, S.B. Lee, Poly(3,4-ethylenedioxythiophene) nanotubes as electrode materials for a high-powered supercapacitor, Nanotechnology 19 (2008) 215710, http://dx.doi.org/10.1088/0957-4484/19/21/215710.

[69] Y. Lu, L. Yeap Foo, Antioxidant activities of polyphenols from sage (*Salvia officinalis*), Food Chem. 75 (2001) 197–202, http://dx.doi.org/10.1016/S0308-8146(01)00198-4.

[70] S.-C. Luo, E. Mohamed Ali, N.C. Tansil, H. Yu, S. Gao, E.A.B. Kantchev, J.Y. Ying, Poly(3,4-ethylenedioxythiophene) (PEDOT) nanobiointerfaces: thin, ultrasmooth, and functionalized PEDOT films with in vitro and in vivo biocompatibility, Langmuir 24 (2008) 8071–8077, http://dx.doi.org/10.1021/la800333g.

[71] A.M. Mohamed, S.N. Metwally, Antiaflatoxigenic activities of some plant aqueous extracts against aflatoxin-B1 induced renal and cardiac damage, J. Pharmacol. Toxicol. 4 (2009) 1–16, http://dx.doi.org/10.3923/jpt.2009.1.16.

[72] B.D. Malhotra, A. Chaubey, S.P. Singh, Prospects of conducting polymers in biosensors, Anal. Chim. Acta 578 (2006) 59–74, http://dx.doi.org/10.1016/j.aca.2006.04.055.

[73] M.K. Manibusan, M. Odin, D.A. Eastmond, Postulated carbon tetrachloride mode of action: a review, J. Environ. Sci. Health C. Environ. Carcinog. Ecotoxicol. Rev. 25 (2007) 185–209, http://dx.doi.org/10.1080/10590500701569398.

[74] M.F. Melzig, G. Bader, R. Loose, Investigations of the mechanism of membrane activity of selected triterpenoid saponins, Planta Med. 67 (2001) 43–48, http://dx.doi.org/10.1055/s-2001-10632.

[75] T. Mosmann, Rapid colorimetric assay for cellular growth and survival: application to proliferation and cytotoxicity assays, J. Immunol. Methods 65 (1983) 55–63.

[76] H. Nakada, The status of development of organic light emitting diodes/organic thin-film transistors, J. Photopolym. Sci. Technol. 20 (2007) 35–38, http://dx.doi.org/10.2494/photopolymer.20.35.

[77] Y.A. Nor, The growth study of Vero cells in different type of Microcarrier, Mater. Sci. Appl. 1 (2010) 261–266, http://dx.doi.org/10.4236/msa.2010.15038.

[78] L. Ouyang, B. Wei, C. Kuo, S. Pathak, B. Farrell, D.C. Martin, Enhanced PEDOT adhesion on solid substrates with electrografted P(EDOT-NH2), Sci. Adv. 3 (2017).

[79] R.M. Owens, G.G. Malliaras, Organic electronics at the Interface with biology, MRS Bull. 35 (2010) 449–456, http://dx.doi.org/10.1557/mrs2010.583.

[80] D. Özerkan, N. Özsoy, E. Yılmaz, Vitamin D and melatonin protect the cell's viability and ameliorate the CCl4 induced cytotoxicity in HepG2 and Hep3B hepatoma cell lines, Cytotechnology 67 (2015) 995–1002, http://dx.doi.org/10.1007/s10616-014-9738-8.

[81] R. Parsons, The electrical double layer: recent experimental and theoretical developments, Chem. Rev. 90 (1990) 813–826, http://dx.doi.org/10.1021/cr00103a008.

[82] F. Poccia, P. Piselli, S. Vendetti, S. Bach, A. Amendola, R. Placido, V. Colizzi, Heat-shock protein expression on the membrane of T cells undergoing apoptosis, Immunology 88 (1996) 6–12, http://dx.doi.org/10.1046/j.1365-2567.1996.d01-656.x.

[83] M. Porres-Martínez, E. González-Burgos, M.E. Carretero, M.P. Gómez-Serranillos, In vitro neuroprotective potential of the monoterpenes α-pinene and 1,8-cineole against H_2O_2-induced oxidative stress in PC12 cells, Z. Naturforsch. C 71 (2016) 191–199, http://dx.doi.org/10.1515/znc-2014-4135.

[84] M. Ravikanth, P. Soujanya, K. Manjunath, T.R. Saraswathi, C.R. Ramachandran, Heterogenecity of fibroblasts, J. Oral Maxillofac. Pathol. 15 (2011) 247–250, http://dx.doi.org/10.4103/0973-029X.84516.

[85] G.A. Rechnitz, D. Coon, C. Babb, A. Ogunseitan, A. Lee, Sensing neuroactive agents in Hawaiian plants, Anal. Chim. Acta 337 (1997) 297–303, http://dx.doi.org/10.1016/S0003-2670(96)00424-2.

[86] K. Rengarajan, S.M. Cristol, M. Mehta, J.M. Nickerson, Quantifying DNA concentrations using fluorometry: a comparison of fluorophores, Mol. Vis. 8 (2002) 416–421.

[87] G. Repetto, A. del Peso, J.L. Zurita, Neutral red uptake assay for the estimation of cell viability/cytotoxicity, Nat. Protoc. 3 (2008) 1125–1131, http://dx.doi.org/10.1038/nprot.2008.75.

[88] S.M. Richardson-Burns, J.L. Hendricks, B. Foster, L.K. Povlich, D.-H. Kim, D.C. Martin, Polymerization of the conducting polymer poly(3,4-ethylenedioxythiophene) (PEDOT) around living neural cells, Biomaterials 28 (2007) 1539–1552, http://dx.doi.org/10.1016/j.biomaterials.2006.11.026.

[89] T. Rodrigues, D. Reker, P. Schneider, G. Schneider, Counting on natural products for drug design, Nat. Chem. 8 (2016) 531–541, http://dx.doi.org/10.1038/nchem.2479.

[90] K.S. Ryu, Y.-G. Lee, Y.-S. Hong, Y.J. Park, X. Wu, K.M. Kim, M.G. Kang, N.-G. Park, S.H. Chang, Poly(ethylenedioxythiophene) (PEDOT) as polymer electrode in redox supercapacitor, Electrochim. Acta 50 (2004) 843–847, http://dx.doi.org/10.1016/j.electacta.2004.02.055.

[91] G. Samuelsson, L. Bohlin, Swedish Academy of Pharmaceutical Sciences, Drugs of Natural Origin: A Treatise of Pharmacognosy, (2009) (Apotekarsocieteten).

[92] F. Sekli-Belaidi, P. Temple-Boyer, P. Gros, Voltammetric microsensor using PEDOT-modified gold electrode for the simultaneous assay of ascorbic and uric acids, J. Electroanal. Chem. 647 (2010) 159–168, http://dx.doi.org/10.1016/j.jelechem.2010.06.007.

[93] P. Sharma, T.S. Bhatti, A review on electrochemical double-layer capacitors, Energy Convers. Manag. 51 (2010) 2901–2912, http://dx.doi.org/10.1016/j.enconman.2010.06.031.

[94] T.A. Skotheim, J.R. Reynolds, Handbook of Conducting Polymers, CRC, 2007.

[95] G.A. Snook, P. Kao, A.S. Best, Conducting-polymer-based supercapacitor devices and electrodes, J. Power Sources 196 (2011) 1–12, http://dx.doi.org/10.1016/j.jpowsour.2010.06.084.

[96] A.N. Sokolov, M.E. Roberts, Z. Bao, Fabrication of low-cost electronic biosensors, Mater. Today 12 (2009) 12–20, http://dx.doi.org/10.1016/S1369-7021(09)70247-0.

[97] S. Srinivasan, Electrode/Electrolyte Interfaces: Structure and Kinetics of Charge Transfer, Fuel Cells, Springer, US, Boston, MA, 2006, pp. 27–92, http://dx.doi.org/10.1007/0-387-35402-6_2.

[98] D.A. Stenger, G.W. Gross, E.W. Keefer, K.M. Shaffer, J.D. Andreadis, W. Ma, J.J. Pancrazio, Detection of physiologically active compounds using cell-based biosensors, Trends Biotechnol. 19 (2001) 304–309, http://dx.doi.org/10.1016/S0167-7799(01)01690-0.

[99] S. Takahashi, T. Abe, J. Gotoh, Y. Fukuuchi, Substrate-dependence of reduction of MTT: a tetrazolium dye differs in cultured astroglia and neurons, Neurochem. Int. 40 (2002) 441–448, http://dx.doi.org/10.1016/S0197-0186(01)00097-3.

[100] M. Thakur, K. Mergel, A. Weng, S. Frech, R. Gilabert-Oriol, D. Bachran, M.F. Melzig, H. Fuchs, Real time monitoring of the cell viability during treatment with tumor-targeted toxins and saponins using impedance measurement, Biosens. Bioelectron. (2012), http://dx.doi.org/10.1016/j.bios.2012.03.024.

[101] I. Tokarev, S. Minko, Multiresponsive, hierarchically structured membranes: new, challenging, biomimetic materials for biosensors, controlled release, biochemical gates, and nanoreactors, Adv. Mater. 21 (2009) 241–247, http://dx.doi.org/10.1002/adma.200801408.

[102] T.A. Tran, M.T. Ho, Y.W. Song, M. Cho, S.K. Cho, Camphor induces proliferative and anti-senescence activities in human primary dermal fibroblasts and inhibits UV-induced wrinkle formation in mouse skin, Phytother. Res. 29 (2015) 1917–1925, http://dx.doi.org/10.1002/ptr.5484.

[103] K. Wang, H. Wu, Y. Meng, Y. Zhang, Z. Wei, Integrated energy storage and electrochromic function in one flexible device: an energy storage smart window, Energy Environ. Sci. 5 (2012) 8384–8389, http://dx.doi.org/10.1039/C2EE21643D.

[104] B. Winther-Jensen, D.R. MacFarlane, New generation, metal-free electrocatalysts for fuel cells, solar cells and water splitting, Energy Environ. Sci. 4 (2011) 2790, http://dx.doi.org/10.1039/c0ee00652a.

[105] S.F. Zakrzewski, S.F. Zakrzewski, Environmental Toxicology, Oxford University Press, 2002.

[106] R. Zang, D. Li, I.-C. Tang, J. Wang, S.-T. Yang, Cell-based assays in high-throughput screening for drug discovery, Int. J. Biotechnol. Wellness Ind. 1 (2012) 31–51.

[107] Z. Zhao, G.F. Richardson, Q. Meng, S. Zhu, H.C. Kuan, J. Ma, PEDOT-based composites as electrode materials for supercapacitors, Nanotechnology 27 (2016) 42001, http://dx.doi.org/10.1088/0957-4484/27/4/042001.